JAERI-M
89-164

HIGH β_p BOOTSTRAP TOKAMAK REACTOR

October 1989

Mitsuru KIKUCHI

日本原子力研究所
Japan Atomic Energy Research Institute

JAERI-M レポートは，日本原子力研究所が不定期に公刊している研究報告書です。
入手の問合わせは，日本原子力研究所技術情報部情報資料課（〒319−11 茨城県那珂郡東海村）あて，お申しこしください。なお，このほかに財団法人原子力弘済会資料センター（〒319-11 茨城県那珂郡東海村日本原子力研究所内）で複写による実費頒布をおこなっております。

JAERI-M reports are issued irregularly.
Inquiries about availability of the reports should be addressed to Information Division, Department of Technical Information, Japan Atomic Energy Research Institute, Tokai-mura, Naka-gun, Ibaraki-ken 319-11, Japan.

編集兼発行　日本原子力研究所
印　　刷　山田軽印刷所

High βp Bootstrap Tokamak Reactor

Mitsuru KIKUCHI

Department of Large Tokamak Research
Naka Fusion Research Establishment
Japan Atomic Energy Research Institute
Naka-machi, Naka-gun, Ibaraki-ken

(Received September 29, 1989)

Basic characteristics of a steady state tokamak fusion reactor is presented. The minimum required energy multiplication factor Q is found to be 20 to 30 for the feasibility of the fusion reactor. Such a high Q steady state tokamak operation is possible, within our present knowledge of the operational constraints and the current drive physics, when a large fraction of the plasma current is carried by the bootstrap current.

Operation at high βp ($\geqq 2.0$) and high $q\psi$ ($= 4 - 5$) with relatively small $\varepsilon\beta p$ (< 0.5) enables to drive bootstrap current up to 70 - 80% of the total plasma current without deteriorating Troyon beta limit. The rest of the plasma current can be driven by the high energy neutral beam with the energy multiplication factor Q of 30 - 50. The energy confinement scaling laws predict that the reactor condition is attainable by increasing the major radius (R_p) up to 9m in such a high βp and high q plasma at relatively low plasma current of 12 MA with the confinement enhancement factor of 2 compared with the L-mode scaling.

This high βp reactor has a reasonable size ($Vp = 1500\ m^3$) and fusion output power (2.5 GW) and is consistent with the present knowledges of the plasma physics of the tokamak, namely the Troyon limit, the energy confinement scalings, the bootstrap current, the current drive efficiency (NB current drive with the total power of 70 MW and the beam energy of 1 MeV) with a favorable aspect on the formation of the cold and dense diverter plasma-condition.

From the economical aspect of the tokamak fusion reactor, a more compact reactor is favorable. The use of the high field magnet with

Bmax = 16T (for example T_i-doped Nb_3Sn conductor) enables to reduce the total machine size to 50% of the above-described conventional design, namely Rp = 7m, Vp = 760 m^{-3}, P_F = 2.8 GW.

Keywords: Bootstrap, Steady State, Reactor, Tokamak

高β_Pブートストラップトカマク炉

日本原子力研究所那珂研究所臨界プラズマ研究部
菊池　満

（1989年9月29日受理）

定常トカマク核融合炉の基本特性を示した。必要な最小エネルギー増倍率Qは核融合炉の成立性のためには20から30が必要である。このような高Qの定常トカマク炉は，現在の運転制約条件と電流駆動の物理の範囲では，プラズマ電流の大部分がブートストラップ電流により駆動される時に可能となる。高β_P($\geqq 2.0$)及び高q_ψ（＝4－5）で比較的小さな$\varepsilon\beta_P$（＜0.5）で運転することにより，トロヨンベータ限界を越えることなくプラズマ電流の70－80％をブートストラップ電流で駆動することができる。プラズマ電流の残りは，高エネルギー中性粒子入射により駆動でき，Q値は30－50が達成できる。エネルギー閉じ込め則からは，主半径を9mに増すことによりI_P＝12MAでLモードの2倍の閉じ込めで核融合炉条件が達成される。この高β_P炉は，適度の大きさ（1500 m^3)と，核融合出力（2.5GW)をもち，現在のトカマクのプラズマ物理の知識と整合性がある。即ち，トロヨン限界，エネルギー閉じ込め則，ブートストラップ電流，電流駆動効率（1MeVビームエネルギーで70MWのNB電流駆動）の知識と整合性をもつ。また，低温高密度ダイバータプラズマの形成に対して良好な側面をもっている。

トカマク炉の経済的観点からは，よりコンパクトな核融合炉が望ましいが，最大磁場B_{max}＝16Tの強磁場コイル（例えばT_i含有$N_{b3}S_n$導体）を用いると，上記設計の半分の装置サイズに減少できる。即ちR_P＝7m，V_P＝760 m^3，P_F＝2.8GWが可能となる。

那珂研究所：〒311-01　茨城県那珂郡那珂町大字向山801－1

目　　次

Contents

1. INTRODUCTION

The design study of the commercial fusion reactor based on the tokamak concept has been made by many authors [1,2]. However such reactor designs assumed larger β_t compared with the Troyon limit or higher current drive efficiency compared with the theories and experiments with fairly optimistic confinement scalings in the limiter configuration. Recent reactor designs such as ITER [3] adopted the higher I_p operation (22-28 MA) to improve the energy confinement which increases the required current drive efficiency of the reactor by an order of magnitude compared with the present experimental result. In the steady state operation of the ITER, the energy multiplication factor Q is 5-10 which is fairly lower than the reactor requirement. The development of the efficient and reactor-relevant current driver is the most important issue to realize the steady state tokamak fusion reactor. The current drive with the lower hybrid wave has been studied extensively after the noble work by Fisch [4]. Despite the improvement of the current drive efficiency in JT-60 [5], the lower hybrid wave is thought to be applicable to the peripheral current drive in high temperature reactor due to the poor wave penetration into the plasma core and the wave absorption by the α particles[6,7,8]. Recent observation of the bootstrap current in TFTR [9] provides a renewed interest on the stationary tokamak based on the bootstrap current. In particular, up to 80% of the plasma current is driven by the bootstrap current in JT-60 [10]. Attainment of such a high bootstrap fraction of the plasma current can influence the reactor design significantly. Since Bickerton pointed out the importance of the bootstrap current in a tokamak[11], there are many important progresses of the understanding of the operational constraints in a tokamak fusion reactor. Especially, the Troyon relation forces to operate at low $<\beta_t>$ so as to increase the bootstrap current. Here we summarize such constraints and show an example of a steady state tokamak fusion reactor which can be realized with relatively low current drive efficiency. The design constraints are summarized in the following section. In section 3, the parameters of the steady state tokamak fusion reactor are described. The discussion and the conclusions are given in section 4.

2. OPERATIONAL CONSTRAINTS

2.1 CRITICAL BETA

The maximum attainable toroidal beta ($<\beta_t> = 4\mu_o<nT>/B^2$) is well expressed by the Troyon relation [12] as follows,

$$<\beta_t> (\%) = g \frac{I_p}{a_p B_t} \tag{1}$$

where, I_p , B_t , a_p and g are the plasma current (MA), the toroidal field (T), the plasma minor radius (m) and the Troyon factor, respectively. The Troyon factor g of 2.7-3.5 has been obtained in both experiments [13] and calculations [14]. Combination with the definition of the β_p gives a well - known relation,

$$\beta_p = \frac{4}{\mu_0 I_p^2 R_p} \int PdV \tag{2}$$

$$\beta_p <\beta_t> = \frac{g^2 \kappa}{4} \tag{3}$$

where κ is the plasma elongation. The equation (3) means that the toroidal beta value $<\beta_t>$ becomes fairly low if we choose the high beta poloidal value β_p to increase the bootstrap current. Therefore, a high field tokamak with relatively high aspect ratio is favorable with our present superconducting materials to keep the plasma pressure and the fusion power density high (see section 2-5).

Figure 1 shows the ($<\beta_t>$, β_p) diagram showing the operational points of various tokamaks. Operational points for ITER[15], NET[16], FER[17] and SSTR (Steady State Tokamak Reactor described in the following section) are shown. The Troyon factor for the total plasma stored energy of 3.5 is used for the reference design of SSTR. Another important limitation on the plasma pressure is observed experimentally at high q and high β_p regime given by $\varepsilon\beta_p <$ C where C is a constant around 0.7-1.1 [18,19] . But there is a quite interesting plasma regime in such a high q and high β_p regime. The numerical analysis shows that there is a possibility to enhance the β limit in high q regimes by increasing the central q value [20]. Indeed the central q value increases above 1.0 with increasing bootstrap current.

The beam driven current and the bootstrap current profiles and the plasma equilibrium are calculated self-consistently with the numerical code [21] in which the α particle pressure is also calculated for a given temperature and density profiles. Figure 2(a) shows a typical example of the current and the safety factor profiles where 73 % of the total plasma current is driven by the bootstrap current. The central safety factor q_0 of 1.7 can be attained while keeping a large magnetic shear in high q operation. The control of the central safety factor q_0 can easily be made through the control of the beam deposition profile. Fig. 2 (b) shows safety factor profiles with varying beam cross section. As is clear from the figure, the central q value can be controlled only by the beam driven current.

The effect of increasing q_0 on the $n= \infty$ ballooning stability is calculated for standard SSTR equilibria. Fig.3 shows the equilibrium configurations, pressure and safety factor profiles, radial profile of the pressure gradient and the S-α diagram for various q_0 values ((3a); $q_0 = 1.0$, (3b) $q_0 = 1.4$, (3c); $q_0 = 1.5$, respectively). In this case, the average toroidal beta $<\beta_t>$ of 3 % (the Troyon factor of 4.0) is stable to the ballooning mode. The control of the q_0 is very effective in enhancing the ballooning limit. Most dangerous low toroidal mode number (n = 1,2,3) MHD instabilities may also be stabilized if a conducting wall is placed at 1.2 times the plasma minor radius[22]. Such a high q reactor seems to be advantageous compared with the low q reactor to decrease the statistical probability of the plasma disruption. Higher plasma elongation is favorable so as to increase plasma pressure limit and the energy confinement. However, there is a maximum plasma elongation in order to maintain vertical plasma stability. The vertical plasma stability is assured when the passive index n_s $(= I_p(\partial M_{ps}/\partial z)^2/(2\pi B_z L_s))$ of the stabilizer is greater than the absolute of the n index ($n_s + n > 0$). The passive index n_s is reduced for the high β_p equilibrium due to increased B_z/I_p . Moreover more negative n index (<< 0) is needed to produce the elongated plasma for the high aspect ratio tokamak. Thus a relatively moderate plasma elongation may be optimum to maintain vertical plasma stability for the large aspect ratio and high β_p tokamak. It should be noted also that the maximum Troyon factor g decreases when $\kappa > 2.0$.

2.2 THE BOOTSTRAP CURRENT

With the accumulations of the experimental evidences showing the existence of the bootstrap current in tokamaks [9,10,23], it is now well grounded to include the bootstrap current for a reactor design. In order to show the constraint in a simple form, we use the most simple expression for the bootstrap current for a pure hydrogen plasma in a uniform current distribution [24] as follows,

$$I_{bs} = 0.67\, \varepsilon^{0.5}\, \beta_p\, I_p \qquad (4)$$

The plasma β_p should satisfy a constraint in order to drive bootstrap current up to a significant fraction of the total plasma current. Here we choose following constraint to drive 70 % of the total plasma current by taking account of the inefficient current drive due to beam and α particles and the non-uniform current profiles as follows,

$$\varepsilon^{0.5}\, \beta_p = 1.07 \qquad (5)$$

The equations (4) and (5) are based on the Hinton-Hazeltine theory which is valid only for extremely slender and pure electron-ion plasmas. Parameter dependence is fairly different from those calculated from the finite aspect ratio Hirshman-Sigmar theory [25]. Detailed calculations have been made with the Hirshman-Sigmar theory on the bootstrap current with a self-consistent plasma equilibrium. The bootstrap current is calculated directly from the parallel momentum and heat balance equations [10].

$$\langle J.B \rangle = \sum_n eZ_n n_n \langle B.u_{//n} \rangle$$

$$= -\, RB_t n_e T_e \sum_n \frac{T_n}{|Z_n| T_e} [\, L_{31}^n\, \ln P_n' + L_{32}^n\, \ln T_n'\,] \qquad (6)$$

where the bootstrap coefficients L_{31}^n and L_{32}^n are calculated from the following parallel momentum and heat balance equations, power / heating and current drive power) regime in such a high β_p reactor which will be discussed in section 2-6.

2.3 CURRENT DRIVE EFFICIENCY

The non-inductive current drive is the key issue to realize the steady state operation of a tokamak reactor. The design efforts for the next generation tokamaks are placed to increase the plasma current up to 30 MA [28]. In such a high current reactor, very high current drive efficiency η_{CD} ($= n_e I_p R_p / P_{abs}$) more than 2.0×10^{20} $Am^{-2}W^{-1}$ is needed to get a high fusion power multiplication factor Q of more than 20 because the bootstrap current is small in such a low β_p plasma. The current drive with the lower hybrid wave is most promising and well-established scheme among many non-inductive current drivers up to now. The highest current drive efficiency so far obtained is 0.34×10^{20} A m^{-2} W^{-1} during the lower hybrid current drive experiments in JT-60[5] which is far from the above requirement. With the help of the bootstrap current, the required driven current decreases significantly under the constraint eqn. (5). Only 20 - 30 % of the total current driven by the external current driver is sufficient for the reactor. The plasma current in such a high β_p reactor is less than 15 MA. Then the requirement for the current drive efficiency is greatly eased to less than 0.5×10^{20} $Am^{-2}W^{-1}$ which is well within our scope. There are many choices for the current driver to realize such relatively low current drive efficiency, beam , fast wave and lower hybrid wave current drivers. Moreover, it is desirable that the plasma heating and current drive are made by a single equipment to simplify and to reduce the cost of the fusion reactor. The high energy neutral beam current drive based on the negative ion source (NNBI) seems to be a promising tool to heat the plasma and to drive the plasma current in high temperature plasmas. The application of the high energy neutral beam injection to the large tokamak will be tested firstly in JT-60U experiment [29] in 1993 and the physics and the engineering feasibility will be demonstrated. The plan and side views of the NNBI system [30] in JT-60U tokamak are shown in Figure 4. The linear dependence of the neutral beam current drive efficiency on the electron temperature is well established experimentally [18] and the current drive efficiency up to 0.5×10^{20} $Am^{-2}W^{-1}$ can be expected in a plasma whose central electron temperature is more than 30 keV. Moreover, the fueling by the

$$\begin{bmatrix} \mu_1^m & \mu_2^m \\ \mu_2^m & \mu_3^m \end{bmatrix} \begin{bmatrix} \langle B.u_{//m}\rangle + V_{1m} \\ -\frac{2\langle B.q_{//m}\rangle}{5P_m} - V_{2m} \end{bmatrix} = \sum_n \begin{bmatrix} l_{11}^{mn} & l_{12}^{mn} \\ l_{21}^{mn} & l_{22}^{mn} \end{bmatrix} \begin{bmatrix} \langle B.u_{//n}\rangle \\ -\frac{2\langle B.q_{//n}\rangle}{5P_n} \end{bmatrix} \quad (7)$$

where

μ_i^m ; viscosity coefficient

l_{ij}^{mn} ; friction coefficient

$u_{//m}$; parallel flow velocity

$q_{//m}$; parallel heat flow

V_{1m} ; $RB_t[(T_m/e_m)(\ln P_m)'+\Phi']$

V_{2m} ; $RB_t(T_m/e_m)(\ln T_m)'$

Φ ; electrostatic potential

' ; $= \frac{\partial}{\partial\psi}$

$\langle\rangle$; flux surface average

Some comparisons between our numerical analysis and the various theoretical formulas and the application to the JT-60 experiment are given in the reference [10] . Present analysis does not include the bootstrap current driven by the α particle which will enhance the bootstrap current although the α particle pressure is included in the equilibrium analysis.

The beam driven current is calculated by the numerical code [26] in which some improvements are made in comparison with the Start-Cordey theory[27].

The beam driven current is calculated by ,

$$J = J_f\,(1\text{-}F(1\text{-}G)) \quad (8)$$

where J_f , F and G are the fast ion current, electron shielding factor ($\sim Z_b/Z_{eff}$) and the trapped electron correction, respectively. The evaluation of the fast ion current is based on the analytical Fokker-Planck solution in which energy diffusion, bounce average effect and particle trapping are included [26]. More complete theoretical and numerical base will be published [21].

For the reference parameters of SSTR, up to 70 % of the total plasma current is driven by the bootstrap current and the rest of the plasma current is carried by the beam driven current. The required neutral beam power is fairly small (70MW) due to the high plasma temperature and the small required driven current. The energy confinement improvement of two times the L-mode is needed to reach high fusion power multiplication factor Q (= fusion output neutral beam is very desirable to compensate the fusion burn up of the deuterium and tritium. In the reference design of the SSTR, the fusion power multiplication factor Q without including the tritium breeding reaction in the blanket can be up to 30 (Q of 50 can be attainable for $\beta_p = 2.2$ (see equilibrium shown in Figure 3)) which is enough for the commercial fusion reactor. The particle fuelling at the plasma center with the energetic neutral beam is one third of the D-T burn up rate for the reference design of the SSTR.

2.4 ENERGY MULTIPLICATION FACTOR

For a steady state tokamak fusion reactor producing net electric power, the energy multiplication factor Q ($= P_F/P_{CD}$, P_F ; total fusion output , P_{CD}; current drive power) must be higher than a certain value in order to get a reasonable plant efficiency η_{plant} ($\eta_{plant} = P_e/P_{th}$, P_e; net electric power, P_{th};total thermal power) of the fusion reactor. The power balance of the fusion plant can be described as follows,

$$P_e = \eta_{th}P_{th} - P_{aux} - P_{eCD} \tag{9}$$

$$P_{aux} = \eta_{aux} P_{th} \tag{10}$$

$$P_{th} = \gamma_{blanket}P_F + P_{CD} \tag{11}$$

$$P_{eCD} = P_{CD}/\gamma_{CD} \tag{12}$$

where, η_{th} , P_{aux}, P_{eCD}, η_{aux} , $\gamma_{blanket}$ and P_{CD} and γ_{CD} are the thermal conversion efficiency, electrical power for the operation of auxiliary systems (for example reactor cooling, vacuum pumping, He refrigeration etc.), electric power for the current drive system, efficiency of the auxiliary power, energy multiplication factor of the blanket, current drive power and power conversion efficiency of the current driver, respectively. Thus the plant efficiency of the steady state tokamak reactor is given by,

$$\eta_{plant} = P_e/P_{th} = \eta_{th} - \eta_{aux} - \frac{1}{\gamma_{CD}(Q\gamma_{blanket}+1)} \tag{13}$$

Figure 5 shows the plant efficiency as a function of the energy multiplication factor Q. As is clear from the figure, Q of 20-30 is required to get the plant efficiency of 20-25 %. The calculations of the current drive efficiency in the reactor parameter with LHCD&FWCD [31] and NBCD [32] show that the maximum attainable energy multiplication factor Q is limited to ~ 5 with our present knowledges of the plasma physics for the standard reactor parameters. In the recent current drive scheme in ITER, Q of 5 is expected by the combination of LHCD for the peripheral current drive and NBCD for the central current drive [15]. The effect of the bootstrap current for enhancing energy multiplication factor Q is shown in figure 6 where the plant efficiency η_{plant} , the energy multiplication factor Q and the driven plasma current by the active current driver $I_p(CD)$ are plotted as a function of the plasma current while keeping the reference SSTR geometry given in table 1 and the Troyon factor g = 3.5. Here the current drive efficiency η_{CD} ($=I_p(CD)n_eR_p/P_{CD}$) is assumed 5×10^{19} MAm^{-2}/MW. Other parameters are same as Figure 5. The acceptable range of the plasma current is fairly large because of the weak dependence of the plant efficiency on the energy multiplication factor. It should be noted that the attainment of the high thermal conversion efficiency η_{th} is more important to realize the economical tokamak reactor.

2.5 GEOMETRICAL CONSTRAINT

The most important geometrical constraint comes from the requirement for the neutron shielding and the tritium breeding blanket in the small major radius side. Here we use the minimum separation of 1.3m between 12T ($N_{b3}S_n$) superconductor and the plasma surface. Then the most important geometrical constraint for the toroidal field B_t at the plasma center is given as follows,

$$B_t = B_{max}(R_p - a_p - 1.3)/R_p \qquad (B_{max} = 12\ \mathrm{T}) \qquad (14)$$

This toroidal field together with the Troyon relation determines the maximum plasma pressure and hence the maximum fusion power density. A large aspect ratio tokamak is favorable to increase the toroidal field at the plasma center so as to compensate the low $<\beta_t>$ operation in such a high β_p reactor. The increase of the maximum toroidal field B_{max} up to 16 T may be possible when the future progress on the superconductor development is successful [33]. In such a high B_{max} tokamak, the Troyon factor g can be reduced to 2.6 which is desirable to reduce the disruption probability. If the g factor of 3.5 is acceptable with careful current profile control in such a high q reactor, the machine size can be reduced which will be discussed in section 3.

2.6 FUSION POWER DENSITY AND NEUTRON WALL LOADING

Although the detailed calculation of the fusion power density is easily made by taking account of the plasma profiles and the fusion reaction rate, it is better to use the approximate formula of the fusion power density P_f to see a parameter dependence as follows,

$$\begin{aligned} P_f &= 0.01 < n_{i20} T_{ikev} >^2 \\ &= 1.54 < \beta_{DT} >^2 B_t^4 \qquad (MW/m^3) \qquad (15) \end{aligned}$$

where n_{i20} , T_{ikev} and β_{DT} are the ion plasma density and temperature in the units of $10^{20} m^{-3}$ and keV and the D-T toroidal beta value, respectively. Here the coefficient is calibrated for the reference SSTR parameters. The required plasma volume becomes large if the fusion power density is small under the constraints, eqns. (3), (5) and (14). The average neutron wall loading P_n at the mid-plane may be approximated by the following formula,

$$P_n = \frac{P_F}{5\pi^2 a_p^2 A} \qquad (MW/m^2) \qquad (16)$$

where A is the aspect ratio.

There is a certain limit of the maximum neutron wall loading and the maximum neutron fluence. With the present knowledge of the first wall materials, the neutron wall loading of 5 MW/m^2 and the total neutron fluence of 5 MWY/m^2 may be reasonable assumptions even if a large fraction of the thermal plasma energy goes to the diverter region [34]. For the reference design of the SSTR described in section 3, the neutron wall loading is 2.6 MW/m^2 . The improvement of the maximum tolerable neutron fluence more than 10 MWY/m^2 is important to increase the life cycle of the first wall for the commercial reactor.

2.7 ENERGY CONFINEMENT

In order to reach high Q regime in such a high β_p plasma, the confinement enhancement is the most crucial issue under low plasma current condition. The experiments on TFTR [35] and JET [23] show that the maximum confinement enhancement factor (H) up to 3 compared with the L-mode has been obtained in the Supershot and the H modes especially in the low plasma current (high q) regime. Even in the L-mode, weaker I_p dependence ($I_p^{0.5}$) has been shown in high power neutral injection heating in JT-60 [36] which also favours the low current operation in a reactor. The isotope effect on the energy confinement characteristics and the centrally peaked α particle heating profile (hence higher heating effectiveness [37]) may improve the energy confinement in a D-T reactor. Here, we use two L-mode scalings, Goldston (Archen) [38] and Shimomura-Odajima [39]. The isotope effect is included by the multiplier $A_i^{0.5}$ and the effective mass of 2.5 is used. The Shimomura-Odajima scaling gives relatively optimistic predictions compared with the Goldston scaling in the high q and lower aspect ratio regime. The important characteristics of such confinement scalings is the dependence on the aspect ratio. Neo-Alcator scaling [40], Goldston scaling and the ohmic part of the Shimomura-Odajima scaling clearly demonstrate that the energy confinement is improved with increasing major radius which means that the energy confinement is governed by the toroidal instability. But the scaling of the incremental energy confinement time given by Shimomura and Odajima suggests that the incremental energy confinement is governed by completely different physics which is independent of the toroidicity. The energy confinement improves with the major radius but the sensitivity to the aspect ratio (or plasma minor radius) is completely different for both scalings. This difference is caused by a lack of the confinement data base of the high aspect ratio large tokamak (A ~ 4 - 5). The study of the aspect ratio dependence of the energy confinement time seems to be most important so as to optimize the fusion reactor. The energy confinement improvement factor of 2 is enough for both scaling in the reference parameters of SSTR. Details will be given in section 3-1 (see Fig.7).

2.8 COLD AND DENSE DIVERTOR PLASMA CONDITION

In order to reduce the damage of the diverter plate, the plasma temperature in front of the diverter plate must be lowered to a few 10 eV. The formation of the cold and dense diverter plasma is well established experimentally [41]. Using the two point diverter model [42], plasma parameters near the diverter plate and the scrape-off layer are given as follows,

$$n_d = \frac{R\Gamma_s}{u_{//d}} \tag{17}$$

$$T_d = \frac{q_{//s} - \int_0^{L_D} W_R dl}{\gamma R \Gamma_s} \tag{18}$$

$$u_{//d} = \sqrt{\frac{2T_d}{m}} \tag{19}$$

$$n_s = \frac{\Gamma_s}{(R-\sqrt{R^2 - T_s/T_d}\,)u_{//d}} \tag{20}$$

$$T_s = (T_d^{3.5} + \frac{3.5 L_D q_{//s}}{\kappa_{//0}})^{2/7} \tag{21}$$

$$u_{//s} = \frac{\Gamma_s}{n_s} \tag{22}$$

where n_d , T_d , $u_{//d}$, n_s ,T_s and $u_{//s}$ are the electron density, the electron temperature and the parallel flow velocity near the diverter plate (subscript ; d) and the scrape-off layer (subscript ; s), respectively. Here R , Γ_s , $q_{//s}$, L_D , γ, $\kappa_{//0}$ and W_R are the flux multiplication factor, the particle flux , the heat flux , the diverter length , the heat transmission coefficient (= 7.8 for hydrogen), the constant of the parallel heat conduction coefficient (=12.5W/cm/eV$^{7/2}$ for hydrogen) and the radiation power density, respectively. The flux multiplication factor R is a strong function of the diverter plasma density which is modelled in this analysis as follows,

$$R = 1.0 + (R_{max} - 1.0)(1.0 - \exp(-2\times10^{-20}\, n_d\,)) \tag{23}$$

The diverter plasma density n_d is obtained iteratively to match this flux multiplication factor. The evaporation and the sputtering from the diverter plate become serious problems during the long pulse neutral beam heating in large tokamaks. The diverter length L_D which is proportional to qR becomes longer than the usual tokamak designs in such a high q and high aspect ratio tokamak.

As is clear from equation (21), high q and high aspect ratio tokamak is easier to get a temperature gradient along the magnetic field line which directly connected to the formation of the cold and dense diverter condition and to the power handling of the heat load to the diverter plate. For the reference parameters of SSTR, this simplified calculation shows that the dense and cold diverter plasma condition can be maintained when the particle confinement time is around 1 second for total α heating power of 500 MW if the 70 % of the total power is radiated near the diverter plate.

3. HIGH β_P STEADY STATE TOKAMAK REACTOR

3.1 REFERENCE PARAMETERS

Major radius and aspect ratio scans under three constraints ; eqn.(3) (Troyon relation), eqn.(5) (high β_p condition) and eqn.(14) (geometrical constraint) are made to optimize the size of the reactor. Here, we choose relatively moderate elongation $\kappa = 1.8$ to assess the vertical plasma stability by considering the high β_p and large aspect ratio conditions. The confinement enhancement factor required to get Q = 30 regime $<nT>\tau_E = 2.3\text{x}10^{21}$ keV.m^{-3}.sec is given by the equi-contour plots in Fig.7 for Goldston scaling and Shimomura-Odajima scaling. As described in section 2-7, the required confinement enhancement factor decreases with increasing plasma major radius. But the aspect ratio dependence is completely different between the two scalings. Figure 7 also shows the equi-contour plot of the fusion output power P_F. The total fusion output power becomes fairly low (< 2 GW) if the plasma major radius is less than 8 m due to the low β_t condition even if the energy confinement is satisfactorily good. If we consider a tokamak fusion reactor with a net electrical power of 1GW(e) similar to the thermal fission reactors such as PWR (pressurized water reactor) and BWR (boiling water reactor), the fusion output power P_F should be of the order of 3 GW. Here, we choose major and minor radii by 9 m and 2.2 m respectively for the reference parameters of SSTR where both Goldston and Shimomura-Odajima scalings require the confinement enhancement factor of 2 and relatively large total fusion output power can be expected. The plasma current I_p is determined from the constraint eqn. (5) as I_p = 12MA. Figure 8 shows the crosssectional views of the standard SSTR, compact SSTR (see section 3-2) and ITER (International Thermonuclear Experimental Reactor). The poloidal cross section of the toroidal field coil is chosen as that of STARFIRE tokamak [2] for the reference case and is comparable with that of the ITER. The major parameters are given in Table 1. This tokamak is characterized by relatively large aspect ratio and high safety factor. The central temperature is chosen up to 34 keV so that the current drive efficiency becomes high and the thermal stability of the plasma is assured. A highly peaked temperature profile may be obtained due to high q operation of this tokamak. The bootstrap current calculated with the neoclassical theory of Hirshman-Sigmar reaches 8.2 MA. The required power of high energy NB is only 70 MW to drive the rest of the plasma current, 3.7 MA.

Figure 9 shows the confinement trace of SSTR in the ($n_i(0)T_i(0)\tau_E(a)$, $T_i(0)$) diagram for the confinement enhancement factor of 2.0. Shimomura-Odajima scaling gives a more optimistic prediction compared with the Goldston scaling due to low current operation. For the Goldston scaling, the α particle heating power P_α and the fusion output power P_F up to 500 MW and 2.5 GW are expected. The plasma stored energy must be increased 100 times the present maximum plasma stored energy recorded in the JET tokamak [23].

In order to satisfy a cold and dense diverter plasma condition, the particle flux to the diverter must be larger than a critical value. This condition gives a requirement for the particle confinement time. Figure 10 shows a simplified calculation of the diverter and scrape off plasma parameters of SSTR as a function of the particle flux from the main plasma. The particle flux corresponding to the particle confinement time of 1 second is shown by the vertical line in Fig. 10. More sophisticated analysis of the cold and dense diverter plasma condition may be necessary . But the cold and dense diverter plasma condition may be formed easily compared with the conventional tokamak reactor design as discussed in section 2-8.

3.2 COMPACT REACTOR

In order to reduce the size of the reactor, the reduction of the total fusion power or some improvements of the operational constraints should be made. If the aspect ratio scaling is established, the machine parameters can be optimized although a reduction of the total fusion power will come out. For example, the major radius of 7 m and the aspect ratio of 3 may be possible if we use the Shimomura-Odajima scaling. The total fusion output power becomes half of the reference parameters.

As discussed in sections 2-1 and 2-5, there is another possibility to increase the maximum plasma pressure either by increasing the maximum toroidal field up to 16 T or by increasing the Troyon factor up to 4.7. In such an enhanced performance, the major radius of the reactor can be reduced to around 7 m. Fig.11 shows the equi-contour plot of the required confinement enhancement factor and the total fusion output power for such an enhanced performance. The steady state reactor may be possible with the major radius of 7 m. The size of the reactor becomes smaller than that of the STARFIRE [2] as is seen in Figure 8. The major parameters for the compact reactor (SSTR-H) is shown in Table 2 in the case of B_{max}=16T. The confinement trace of the SSTR-H is shown in Figure 12.

4. DISCUSSIONS AND CONCLUSIONS

Basic idea of a steady state tokamak reactor based on the bootstrap current is given with the present knowledges of the operational constraints of the tokamak reactor. Operation of the tokamak at high β_p and high q with relatively small $\varepsilon\beta_p$ enables to drive bootstrap current up to 70-80 % of the total plasma current. The rest of the plasma current can be driven by the high energy neutral beam current drive with the high fusion power multiplication factor Q of up to 30 (Q of 50 if the β_p of 2.2 is attainable either by increasing Troyon factor with the tailoring of the current profile or by increasing maximum B_t). This high β_p tokamak is also stable to the n= ∞ ballooning mode. The major radius of a commercial reactor becomes around 9.0 m in order to produce the total fusion power of 2.5 GW in which the neutron wall loading of 2.6 MW/m^2 is expected and is well within the target range of our present material development for the nuclear fusion. In order to realize such a steady state reactor, the most crucial issue is not the current drive efficiency but the enhancement of the energy confinement time up to 2 times the L-mode which is also well within our scope. Probably the impurity and particle control will become more important issues in such a steady state reactor. A significant reduction of the reactor size becomes possible when an improvement either in the maximum toroidal field or the Troyon factor has been made. Such a high q and high aspect ratio tokamak seems to be favorable to produce cold and dense diverter plasma condition.

The advantages of such a steady state reactor concept can be summarized as follows,

(1) Operation at high β_p drives large bootstrap current and the required current drive efficiency becomes fairly low ($5x10^{19}$ $Am^{-2}W^{-1}$).

factor and the total fusion output power for such an enhanced performance. The steady state reactor may be possible with the major radius of 7 m. The size of the reactor becomes smaller than that of the STARFIRE [2] as is seen in Figure 8. The major parameters for the compact reactor (SSTR-H) is shown in Table 2 in the case of B_{max}=16T. The confinement trace of the SSTR-H is shown in Figure 12.

4. DISCUSSIONS AND CONCLUSIONS

Basic idea of a steady state tokamak reactor based on the bootstrap current is given with the present knowledges of the operational constraints of the tokamak reactor. Operation of the tokamak at high β_p and high q with relatively small $\varepsilon\beta_p$ enables to drive bootstrap current up to 70-80 % of the total plasma current. The rest of the plasma current can be driven by the high energy neutral beam current drive with the high fusion power multiplication factor Q of up to 30 (Q of 50 if the β_p of 2.2 is attainable either by increasing Troyon factor with the tailoring of the current profile or by increasing maximum B_t). This high β_p tokamak is also stable to the n= ∞ ballooning mode. The major radius of a commercial reactor becomes around 9.0 m in order to produce the total fusion power of 2.5 GW in which the neutron wall loading of 2.6 MW/m^2 is expected and is well within the target range of our present material development for the nuclear fusion. In order to realize such a steady state reactor, the most crucial issue is not the current drive efficiency but the enhancement of the energy confinement time up to 2 times the L-mode which is also well within our scope. Probably the impurity and particle control will become more important issues in such a steady state reactor. A significant reduction of the reactor size becomes possible when an improvement either in the maximum toroidal field or the Troyon factor has been made. Such a high q and high aspect ratio tokamak seems to be favorable to produce cold and dense diverter plasma condition.

The advantages of such a steady state reactor concept can be summarized as follows,

(1) Operation at high β_p drives large bootstrap current and the required current drive efficiency becomes fairly low (5×10^{19} $Am^{-2}W^{-1}$).

(2) The high energy neutral beam injection system can be used for both heating and current drive (which reduces the total plant cost).

(3) Heating and current driver can be placed far from the reactor which is desirable for the reliability and the maintenance.

(4) Operation at high q(a) and high q(0) enables the easy access to the second stability regime for the $n = \infty$ ideal ballooning modes with stability against the low n kink-ballooning modes.

(5) Operation at high q decreases the probability of disruptions.

(6) Operation at lower plasma current decreases the disruption forces.

(7) Operation at high q(0) eliminates the sawteeth oscillation of the fusion output power and produces peaked temperature profiles although the disappearance of the sawteeth may increase the accumulation of the impurity.

(8) The high energy neutral beam may be partly useful for the D-T fueling to compensate the fusion burn up of the D-T fuel.

(9) Operation at high q increases the diverter length which helps to form the cold and dense diverter plasma condition.

This concept can be realized with the H mode energy confinement with the confinement enhancement factor of 2. The required plasma current is only 12 MA which is very favorable from the engineering feasibility against the plasma disruption.

The test of this concept will be made in the JT-60 upgrade program [29] using the elongated diverter configuration (A = 4) with relatively small plasma current $I_p = 2.6$ MA.

ACKNOWLEDGEMENTS

The author would like to express his appreciation to Dr. Y. Shimomura for stimulated discussions on the reactor design. The ballooning analysis code and the current drive code provided by Dr's M.Azumi and K.Tani are greatly acknowledged. The author would like to express his appreciation to Drs. M. Yoshikawa, M. Tanaka and S. Tamura for their continuous encouragements.

REFERENCES

[1] CONN, R. W., KULCINSKI, G. L., MAYNARD, C. W. et al., Proc. 7-th Int. Conf. Plasma Physics and Controlled Nuclear Fusion Research, vol.3 (IAEA,Vienna, 1979) 203.

[2] BAKER, C. C., ABDOU, M. A., DEFREECE, D. A., et al., "STARFIRE - a Commercial Tokamak Fusion Power Plant Study ", ANL/FPP-80-1 (1980).

[3] ITER team presented by K.,TOMABECHI, , 12-th Int. Conf. Plasma Physics and Controlled Nuclear Fusion Research, IAEA-CN-50/F-I-4

[4] FISCH, N. J., Phys. Rev. Lett. vol.41(1978)873.

[5] IKEDA, Y., IMAI, T., USHIGUSA, K., et al., to be published in Nuclear Fusion.

[6] ITER team presented by D., POST, 12-th Int. Conf. Plasma Physics and Controlled Nuclear Fusion Research, IAEA-CN-50/F-II-1.

[7] WONG,K.-L., ONO,M., Nuclear Fusion 23 (1983) 805.

[8] WONG,K.-L.,ONO,M.,Nuclear Fusion 24 (1984)615.

[9] ZARNSTORFF,M.C., BELL,M.G.,BITTER,M.,GOLDSTON,R.J. et al., Phys. Rev. Lett. vol.60 (1988) 1306.

[10] KIKUCHI, M., AZUMI, M., TANI, K. and KUBO, H., submitted to Nuclear Fusion.

[11] BICKERTON, R. J., CONNOR, J.W., TAYLOR, J. B. , Nat. Phys. Sci. vol.229 (1971) 110. ; GALEEV, A. A., Sov. Phys.- JETP vol.32 (1971) 752.

[12] TROYON, F., GRUBER, R., SAURENMANN, H., SEMENZATO, S., SUCCI, S. , Plasma Physics and Controlled Fusion vol.26 (1984) 209.

[13] STAMBAUGH, R., D., MOORE, R., W., BERNARD, L., C., KELLMAN, A., G., STRAIT., E., J., et al., Plasma Physics and Controlled Nuclear Fusion Research 1984 (Proc. 10 th Int. Conf. London, 1984), Vol.1, IAEA, Vienna (1984) 217.

ACKNOWLEDGEMENTS

The author would like to express his appreciation to Dr. Y. Shimomura for stimulated discussions on the reactor design. The ballooning analysis code and the current drive code provided by Dr's M.Azumi and K.Tani are greatly acknowledged. The author would like to express his appreciation to Drs. M. Yoshikawa, M. Tanaka and S. Tamura for their continuous encouragements.

REFERENCES

[1] CONN, R. W., KULCINSKI, G. L., MAYNARD, C. W. et al., Proc. 7-th Int. Conf. Plasma Physics and Controlled Nuclear Fusion Research, vol.3 (IAEA,Vienna, 1979) 203.

[2] BAKER, C. C., ABDOU, M. A., DEFREECE, D. A., et al., "STARFIRE - a Commercial Tokamak Fusion Power Plant Study ", ANL/FPP-80-1 (1980).

[3] ITER team presented by K.,TOMABECHI, , 12-th Int. Conf. Plasma Physics and Controlled Nuclear Fusion Research, IAEA-CN-50/F-I-4

[4] FISCH, N. J., Phys. Rev. Lett. vol.41(1978)873.

[5] IKEDA, Y., IMAI, T., USHIGUSA, K., et al., to be published in Nuclear Fusion.

[6] ITER team presented by D., POST, 12-th Int. Conf. Plasma Physics and Controlled Nuclear Fusion Research, IAEA-CN-50/F-II-1.

[7] WONG,K.-L., ONO,M., Nuclear Fusion 23 (1983) 805.

[8] WONG,K.-L.,ONO,M.,Nuclear Fusion 24 (1984)615.

[9] ZARNSTORFF,M.C., BELL,M.G.,BITTER,M.,GOLDSTON,R.J. et al., Phys. Rev. Lett. vol.60 (1988) 1306.

[10] KIKUCHI, M., AZUMI, M., TANI, K. and KUBO, H., submitted to Nuclear Fusion.

[11] BICKERTON, R. J., CONNOR, J.W., TAYLOR, J. B. , Nat. Phys. Sci. vol.229 (1971) 110. ; GALEEV, A. A., Sov. Phys.- JETP vol.32 (1971) 752.

[12] TROYON, F., GRUBER, R., SAURENMANN, H., SEMENZATO, S., SUCCI, S. , Plasma Physics and Controlled Fusion vol.26 (1984) 209.

[13] STAMBAUGH, R., D., MOORE, R., W., BERNARD, L., C., KELLMAN, A., G., STRAIT., E., J., et al., Plasma Physics and Controlled Nuclear Fusion Research 1984 (Proc. 10 th Int. Conf. London, 1984), Vol.1, IAEA, Vienna (1984) 217.

[14] TUDA, T., AZUMI, M., ITOH, K., KURITA, G., TAKEDA, T., et al., ibid. Vol.2, IAEA, Vienna (1984) 173.
[15] ITER team presented by Y.SHIMOMURA., 12-th Int. Conf. Plasma Physics and Controlled Nuclear Fusion Research, IAEA-CN-50/F-II-4.
[16] NET team, in Plasma Physics and Controlled Nuclear Fusion Research 1986 (Proc. 11-th Int. Conf. Kyoto, 1986) vol.3 IAEA, Vienna (1987) 249.
[17] SUGIHARA, M., FUJISAWA, N., IIDA, H., NISHIO, S., SEKI, Y. et al., 12-th Int. Conf. Plasma Physics and Controlled Nuclear Fusion Research, IAEA-CN-50/G-I-2.
[18] McGUIRE, K., ARUNASALAM, V., BELL, M.G., BITTER, M., et al., in Plasma Physics and Controlled Nuclear Fusion Research 1986 (Proc. 11-th Int. Conf. Kyoto, 1986) vol.1 IAEA, Vienna (1987) 421.
[19] SIMONEN, T. C., MATSUOKA, M., BHADRA,D.K., et al., 12-th Int. Conf. Plasma Physics and Controlled Nuclear Fusion Research, IAEA-CN-50/E-3-6.
[20] ANTONSEN,T. BASU, B., COPPI,B., CREW,G., ENGLADE, R., et al., in Plasma Physics and Controlled Nuclear Fusion Research 1980 (Proc. 8-th Int. Conf. Brussels, 1980) vol.1 IAEA, Vienna (1981) 83.
[21] TANI, K., AZUMI, M., DEVOTO, R.S., Numerical Analysis of 2-D MHD equilibrium with Non-inductive Plasma Current in Tokamaks, submitted to J. Comp. Phys.
[22] GERVER, M.J., KESNER, J. and RAMOS, J.J., Phys. Fluids 31(1988) 2674.
[23] BICKERTON,R.J. and the JET team, 12-th Int. Conf. on Plasma Physics and Controlled Nuclear Fusion Research, IAEA-CN-50/A-1-3.
[24] CORDEY, J.G., CHALLIS, C.D. and STUBBERFIELD, P.M., Plasma Physics and Controlled Fusion 30 (1988) 1625.
[25] HIRSHMAN, S. P. , SIGMAR, D. J., Nucl. Fusion 21 (1981) 1079.
[26] TANI, K., SUZUKI, M., YAMAMOTO, S., AZUMI, M., On the Analysis of Beam Driven Current in a Tokamak, Rep. JAERI-M 88-042 (1988).
[27] START, D.F.H. and CORDEY, J.G., Phys. Fluids 23 (1980) 1477.
[28] REBUT, P. H. , 12-th Int. Conf. Plasma Physics and Controlled Nuclear Fusion Research, IAEA-CN-50/I-I-1.

[29] KIKUCHI, M. Ando,T., Araki,M., T.Horie, Horiike,T., et al., ' JT-60 Upgrade Program' , Proc. 15-th Symposium on Fusion Technology (1988, Utrecht) vol.1 (1989) 287.

[30] MATSUOKA, M., KAMADA,Y., KIKUCHI, M.,KURIYAMA,M., KUSAMA,Y. et al., ' Study on Negative Ion Based Neutral Beam Injection System for JT-60 Upgrade ' , JAERI-M 89-117 (in Japanese).

[31] EHST,D.A.,EVANS,K.,Jr., Nuclear Fusion 27 (1987)1267.

[32] YAMAMOTO,S.,OKANO,K., et al., in Plasma Physics and Controlled Nuclear Fusion Research 1986 (Proc. 11-th Int. Conf. Kyoto, 1986) vol.3 IAEA, Vienna (1987)267.

[33] SHIMAMOTO, S., ANDO, T., HIYAMA, T., TSUJI, H., TAKAHASHI, Y., et al., in Plasma Physics and Controlled Nuclear Fusion Research 1986 (Proc. 11-th Int. Conf. Kyoto, 1986) vol.3 IAEA, Vienna (1987) 357.

[34] MAGNETIC FUSION ADVISORY COMMITTEE PANEL X, Report on High Power Density Fusion System (1985).

[35] BELL, M.G., ARUNASALAM, V.,BARNES, C.W., BITTER,M. et al., 12-th Int. Conf. Plasma Physics and Controlled Nuclear Fusion Research , IAEA-CN-50/A-1-2.

[36] KIKUCHI, M., HIRAYAMA, T., SHIMIZU, K., et al., Nucl. Fusion 27 (1987) 1239.

[37] CALLEN, J. D., CHRISTIANSEN, J.P., CORDEY, J.G.,et al., Nuclear Fusion 27 (1987) 1857.

[38] GOLDSTON, R.J., Plasma Physics and Controlled Nuclear Fusion 26(1984) 87.

[39] ODAJIMA.,K. and SHIMOMURA, Y., Energy confinement scaling based on offset linear characteristic , Rep. JAERI-M 88-068 (1988).

[40] EFTHIMION, P.C., BELL, M.G., BLANCHARD, W.R., BRETZ, N., et al., Phys. Rev. Lett. Vol.52 (1984) 1492.

[41] SHIMADA, M., NAGAMI, M.,IOKI, K., IZUMI, S., et al., Nuclear Fusion 22 (1982) 643.

[42] SAITO, S., KOBAYASHI, T., SUGIHARA, M., HIRAYAMA, T. and FUJISAWA, N. , Nuclear Fusion 25 (1985) 828.

Table 1 Machine, plasma and nuclear parameters of the standard SSTR.

· REFERENCE PARAMETERS OF SSTR

PARAMETERS (UNIT)	VALUE
Major Radius R_p (m)	9.0
Minor Radius a_p (m)	2.2
Elongation κ	1.8
Triangularity δ	0.3
Aspect Ratio A	4.1
Plasma Volume V_p (m^3)	1500
Plasma Current I_p (MA)	12
Toroidal Field B_T (T)	7.33
Safety Factor q_{eff}	5.
Toroidal Beta $\langle\beta_t\rangle$ (%)	2.55
DT Beta $\langle\beta_{DT}\rangle$ (%)	1.9
Poloidal Beta β_p	2.0
Troyon Factor g	3.5
Average DT Density $\langle n_{DT}\rangle$ (m^{-3})	7.6×10^{19}
Average Density $\langle n_e\rangle$ (m^{-3})	8.9×10^{19}

PARAMETERS (UNIT)	VALUE
Average Thermal Pressure $\langle nT\rangle$ ($keVm^{-3}$)	13.8×10^{20}
Pressure Peaking Factor $\frac{n(0)T(0)}{nT}$	3
Central Temperature T(0)(keV)	34
Bootstrap Current I_{bt} (MA)	8-9
Beam Driven Current I_p^b (MA)	3-4
NBI Power P_{NB} (MW)	70
Beam Energy E_b (MeV)	1.0 (D^0) 1.2 (T^0)
Fusion Power P_F (GW)	2.5
Fusion Power Density P (MW/m^3)	1.7
Neutron Wall Loading P_n (MW/m^2)	2.6
α-Particle Power P_α (GW)	0.5
Plasma Energy W_s (MJ)	1300
Power Gain Q	30
Fuel Burn Rate $\dot{N}_{DT}^b$ (sec^{-1})	1.8×10^{21}
Fuelling Rate $\dot{N}_f$ (sec^{-1})	4×10^{20}

PARAMETERS (UNIT)	VALUE
Particle Confinement Time τ_p (sec)	1.0
Particle Outflux Γ_{out} (sec^{-1})	1.3×10^{23}
Divertor Length L_D (m)	20
Scrape off Density n_s (m^{-3})	6×10^{19}
Divertor Density n_d (m^{-3})	2×10^{20}
Scrape off Temperature T_s (eV)	200
Divertor Temperature T_d (eV)	30
Scrape off Thickness δ (m)	0.04
Flux Multiplication R_M	30
Particle Flux Ratio $\frac{\Gamma_{out}}{S_\alpha}$	140

$n_e = n_{eo}(1-(r/a)^2)^{0.5}$, $T_e = T_{eo}(1-(r/a)^2)^{1.5}$ assumed.

Table 2 Machine , plasma and nuclear parameters of the compact SSTR .

SSTR - H

PARAMETERS (UNIT)	VALUE
Major Radius R_p (m)	7.0
Minor Radius a_p (m)	1.75
Elongation K	1.8
Triangularity δ	0.3
Aspect Ratio A	4.0
Plasma Volume V_p (m^3)	760
Plasma Current I_p (MA)	12
Toroidal Field B_T (T)	9
Safety Factor q_{eff}	5.0
Toroidal Beta $\langle\beta_t\rangle$ (%)	2.55
DT Beta $\langle\beta_{DT}\rangle$ (%)	1.9
Poloidal Beta β_p	2.0
Troyon Factor g	3.5
Average DT Density $\langle n_{DT}\rangle$ (m^{-3})	11.6×10^{19}
Average Density $\langle n_e\rangle$ (m^{-3})	13.5×10^{19}

PARAMETERS (UNIT)	VALUE
Average Thermal Pressure $\langle nT\rangle$ ($keVm^{-3}$)	21×10^{20}
Pressure Peaking Factor $\frac{n(0)T(0)}{\langle nT\rangle}$	3
Central Temperature T(0)(keV)	34
Bootstrap Current I_{bt} (MA)	8-9
Beam Driven Current I_p^b (MA)	3-4
NBI Power P_{NB} (MW)	80
Beam Energy E_b (MeV)	1.0 (D^0) 1.2 (T^0)
Fusion Power P_F (GW)	2.8
Fusion Power Density P(MW/m^3)	3.7
Neutron Wall Loading P_n (MW/m^2)	4.6
α-Particle Power P_α (GW)	0.56
Plasma Energy W_s (MJ)	880
Power Gain Q	35
Fuel Burn Rate $\dot{N}_{DT}^b$ (sec^{-1})	2.0×10^{21}
Fuelling Rate $\dot{N}_f$ (sec^{-1})	5×10^{20}

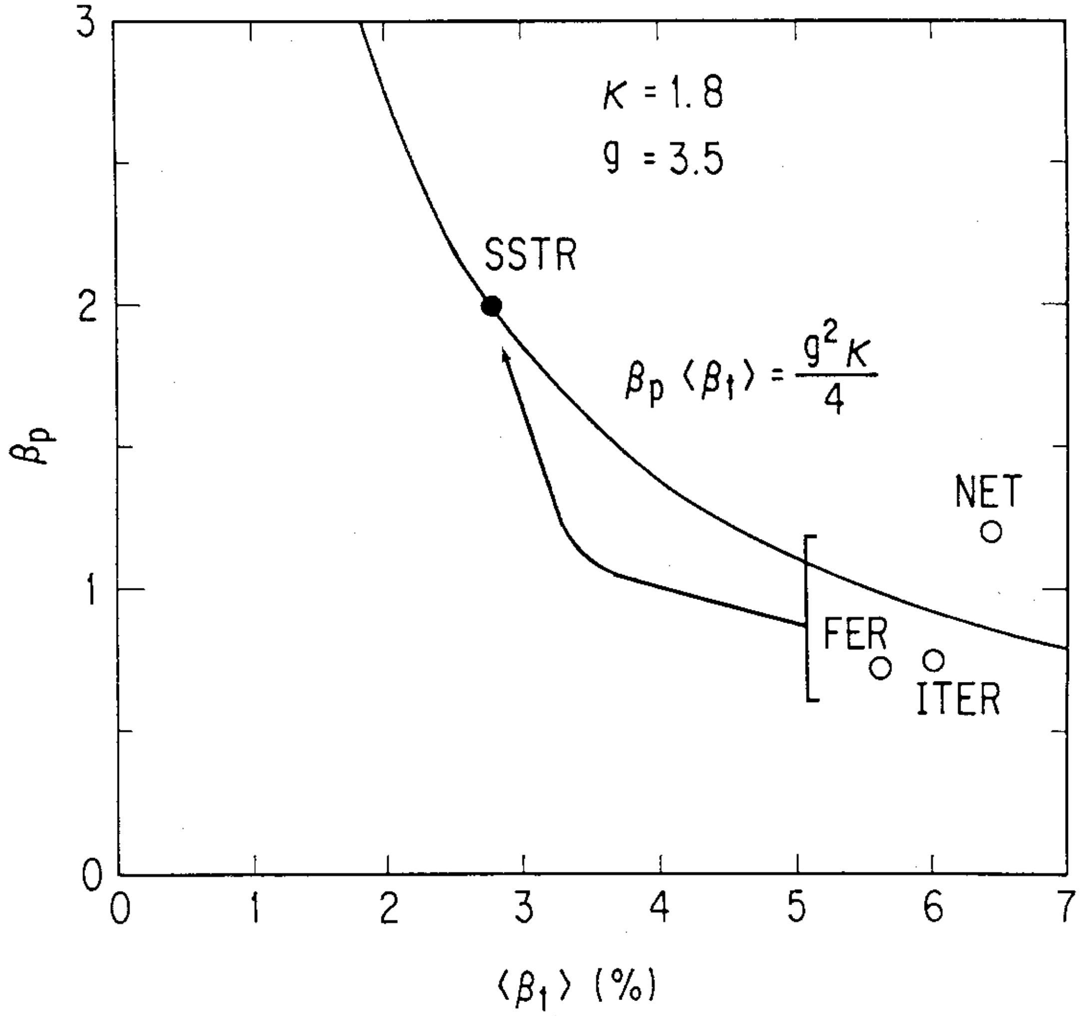

Fig. 1 ($<\beta_t>$, β_p) diagram showing the Troyon relation. The solid line shows the equation (3) with $\kappa = 1.8$ and $g = 3.5$. Operational points of ITER, NET, FER and SSTR are shown. SSTR is characterized by the high β_p operation compared with the next generation tokamaks.

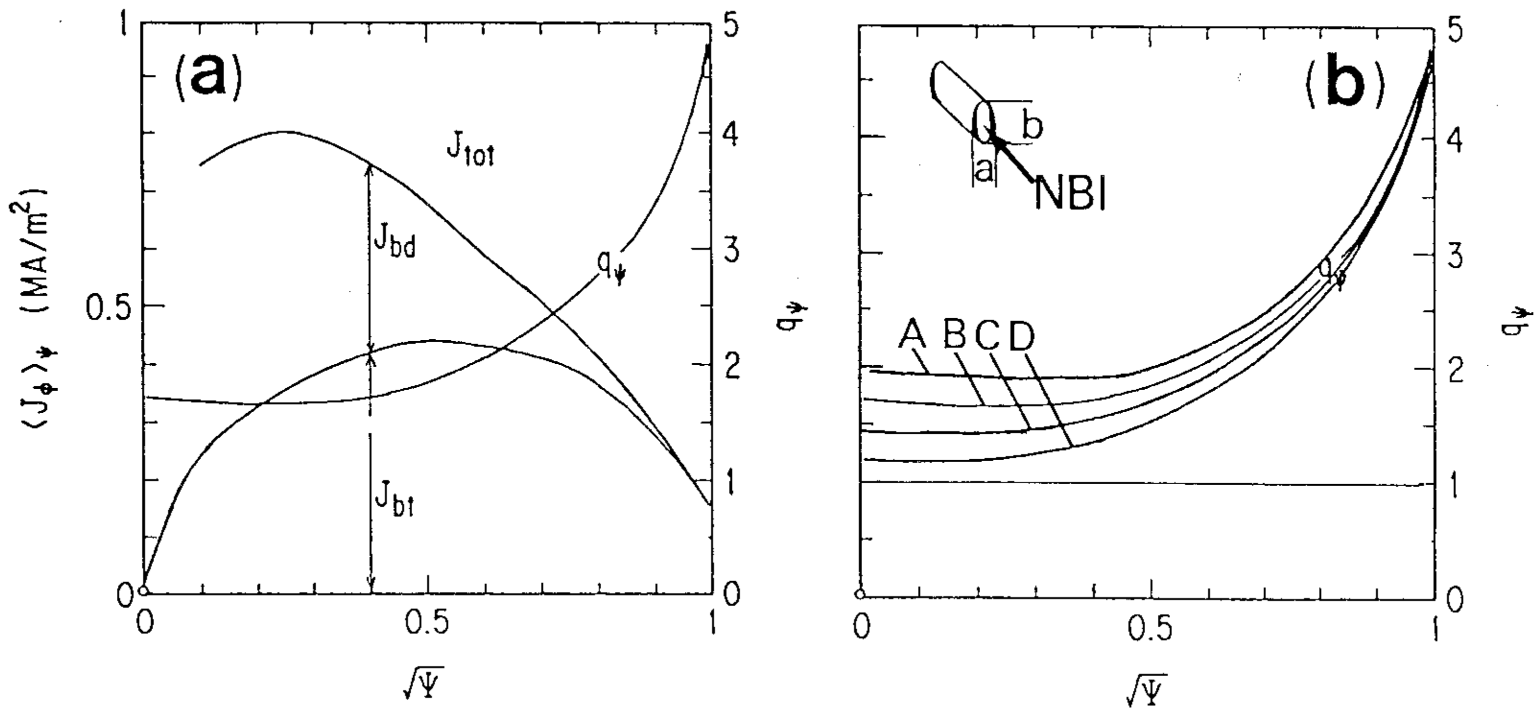

Fig.2 (a) The current density and the safety factor profiles of a steady state tokamak whose current are carried by the bootstrap current (8.8 MA) and the beam driven current (3.2 MA). Without the beam driven current, the current profile becomes hollow which is unstable to the double tearing instability. High energy neutral beam is suitable to drive plasma current at the plasma center. Parameters are same with those given in Table 1. (b) The safety factor profiles with varying beam cross section. (A) a = 2 m, (B) a = 1.8 m, (C) a = 1.6 m, (D) a = 1.4 m. b/a = 2.0 for all cases.

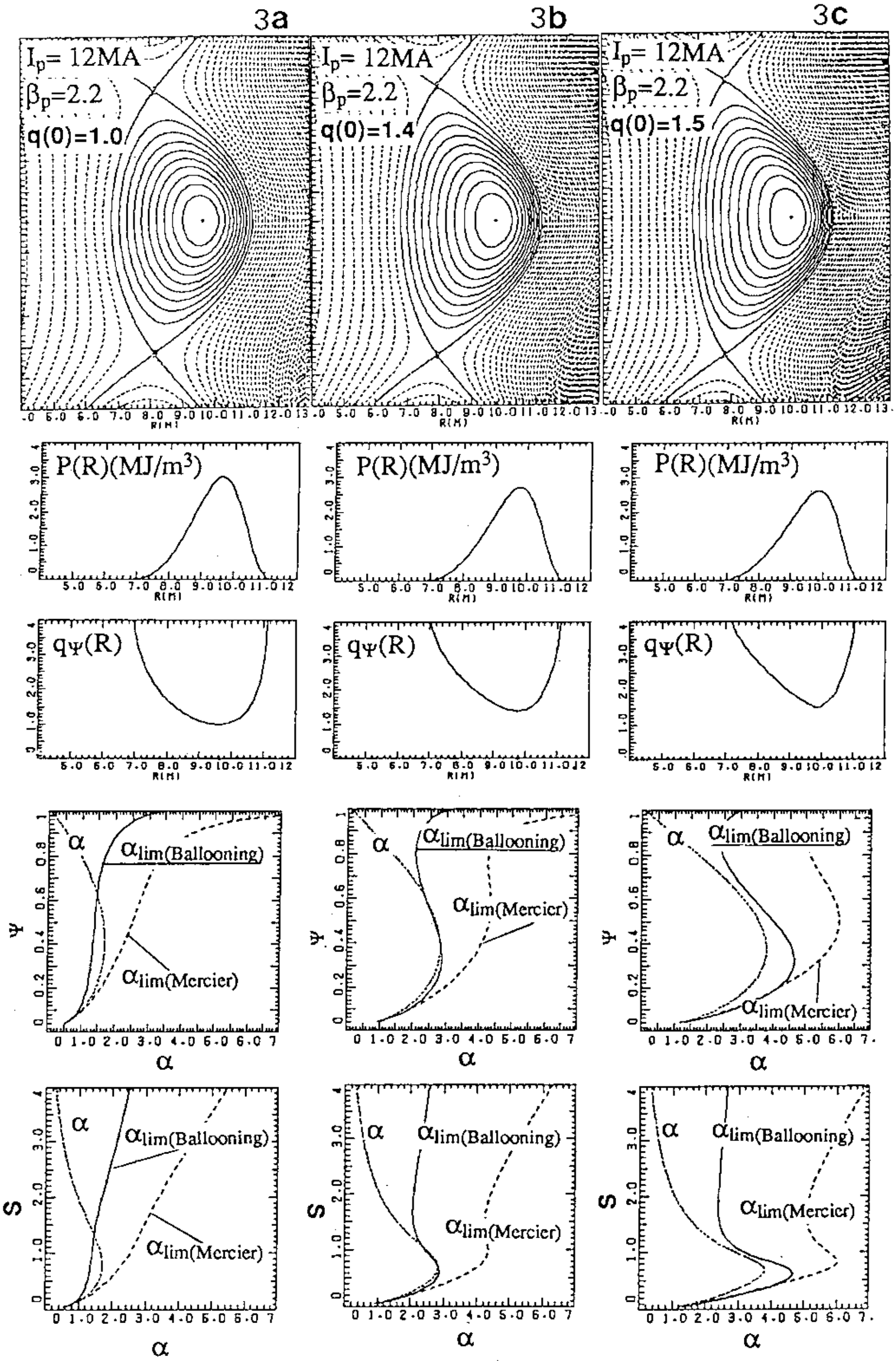

Fig.3 Equilibrium configurations, pressure (P(R)) and safety factor (q(R)) profiles, pressure gradient profile($\alpha(\psi)$) and S-α diagrams for various q(0) values ((3a); q(0)=1.0, (3b); q(0)=1.4, (3c); q(0)=1.5). Here the definitions of S and α are $S=r(dq/dr)/q$, $\alpha=-2Rq^2(dP/dr)/B^2$,respectively. The minor radius r is defined by $r=\sqrt{V(\Psi)/(2\pi^2R_0)}$ (V is the volume inside the flux surface). The MHD limit of the pressure gradient α_{lim} is also given for the ballooning and Mercier modes in the figure. The equilibrium becomes stable to ballooning and Mercier modes when q(0)>1.5.

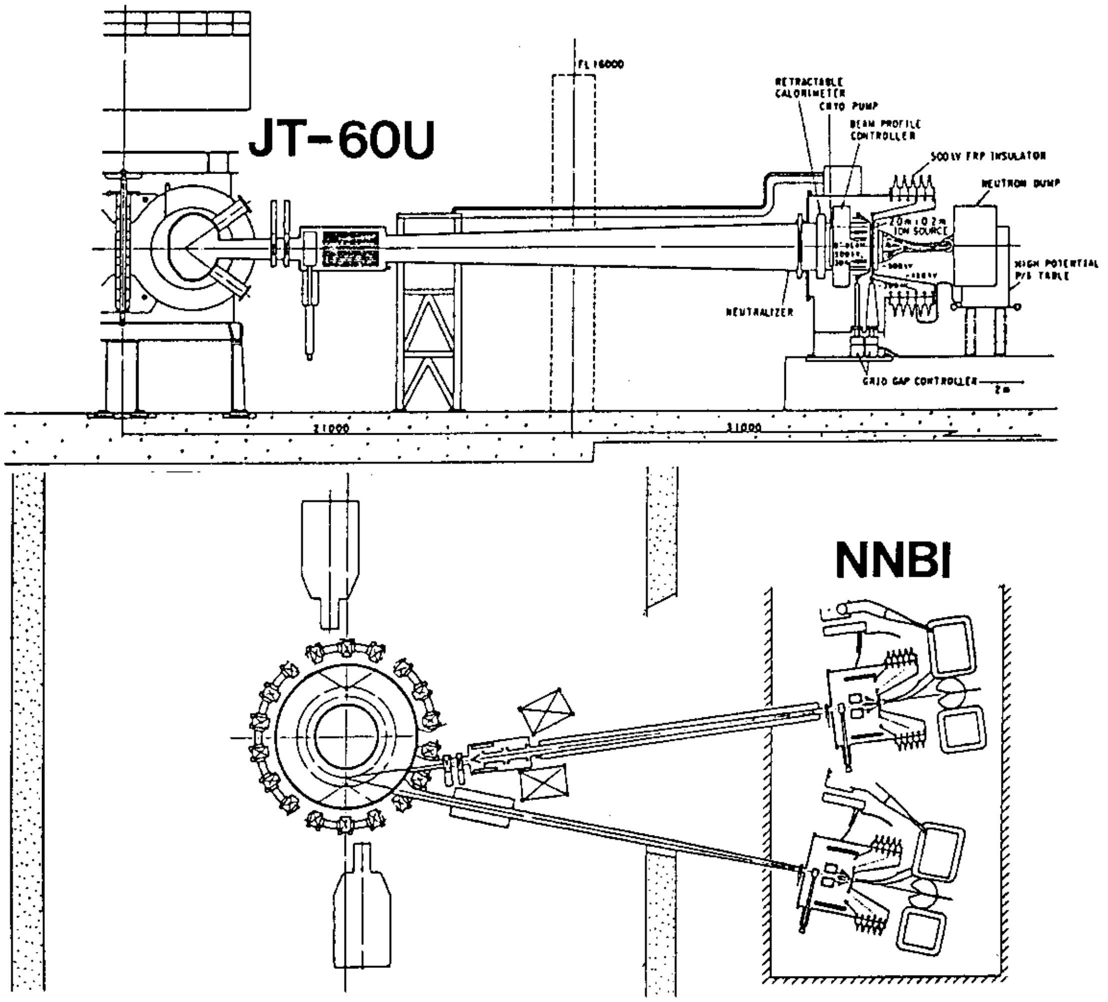

Fig.4 Schematic views of NNBI system in JT-60U. NNBI system will attain the beam energy E_b=500 keV (P_b=10MW) by the end of 1994.

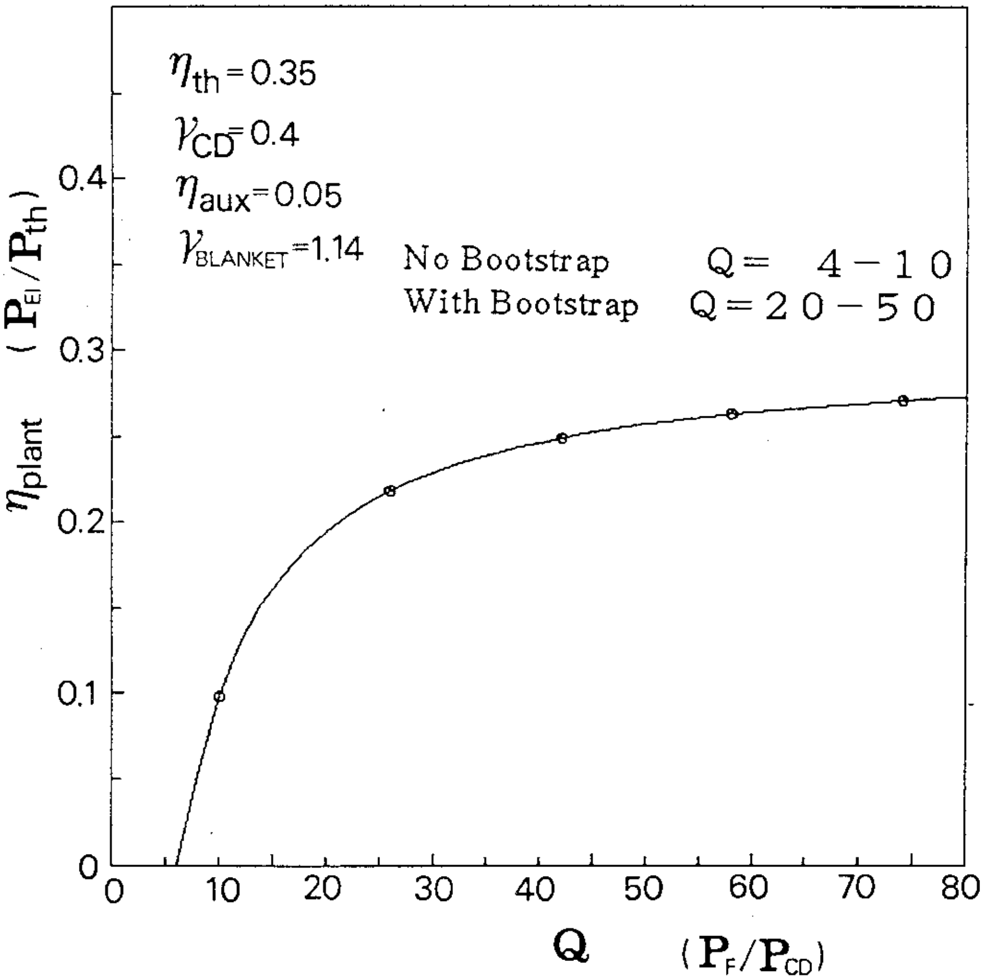

Fig.5 The plant efficiency of the tokamak fusion reactor as a function of the energy multiplication factor Q.

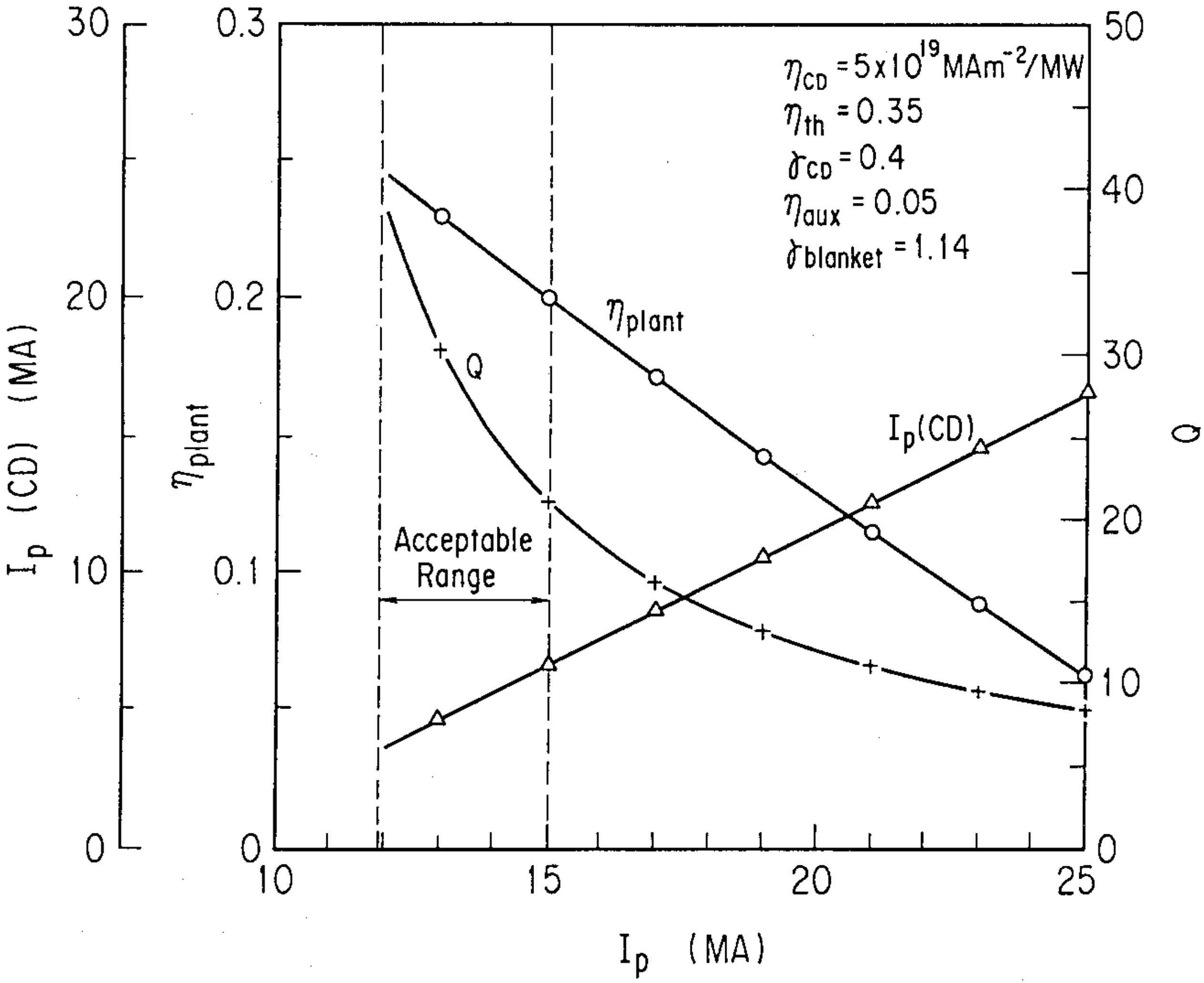

Fig.6 The plant efficiency (η_{plant}), the energy multiplication factor (Q) and the actively driven current ($I_{p(CD)}$) for the steady state reactor as a function of the plasma current for the reference SSTR geometry with fixed Troyon factor.

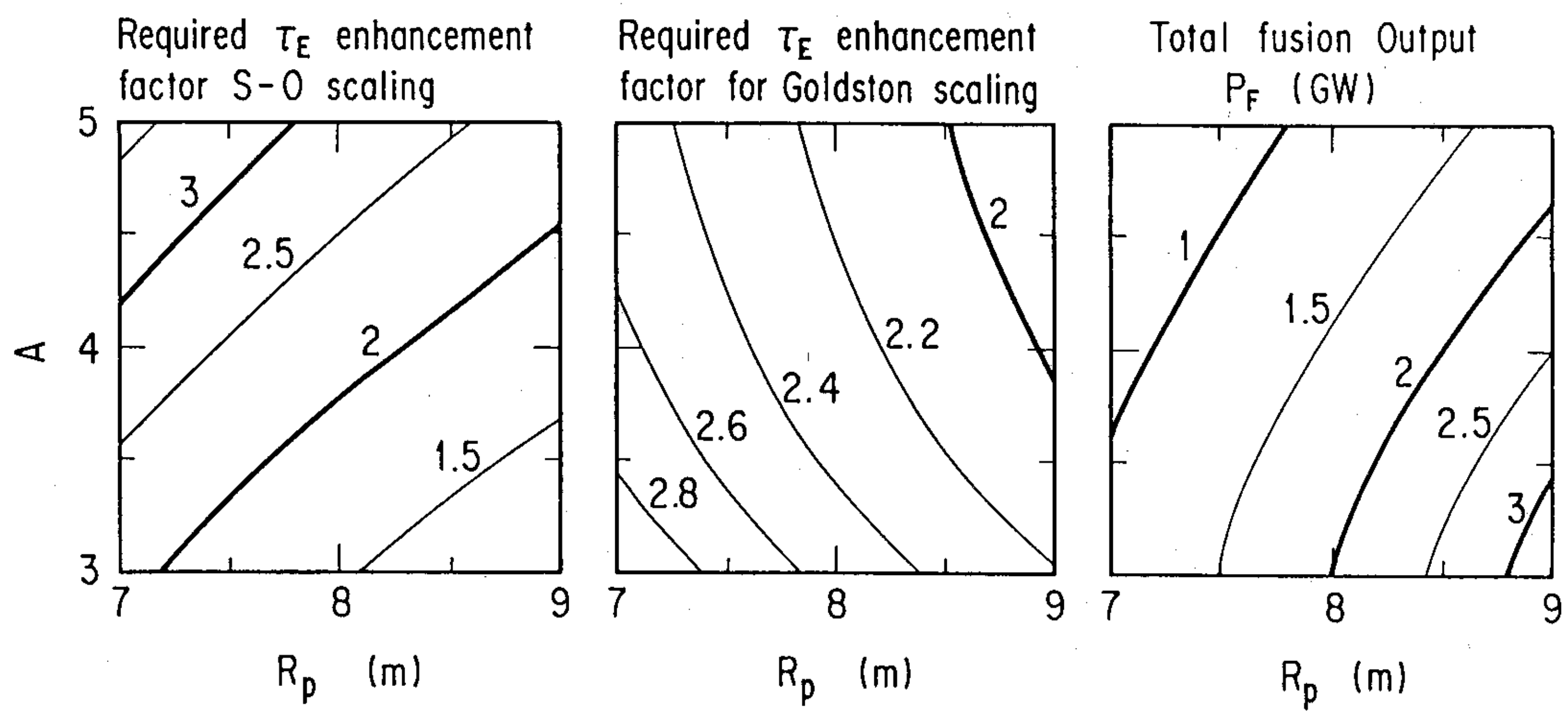

Fig.7 Equi-contour plots of the required enhancement factor of the energy confinement as a function of the major radius and the aspect ratio for Goldston scaling and Shimomura-Odajima scaling to get Q = 30 condition. The fast ion and α particle fraction of the plasma stored energy is calculated to be 23 % and the fuel ion density is assumed 85.7 % of the electron density. The Troyon factor of 3.5 is assumed for total plasma energy. The maximum toroidal field of 12 T is assumed.

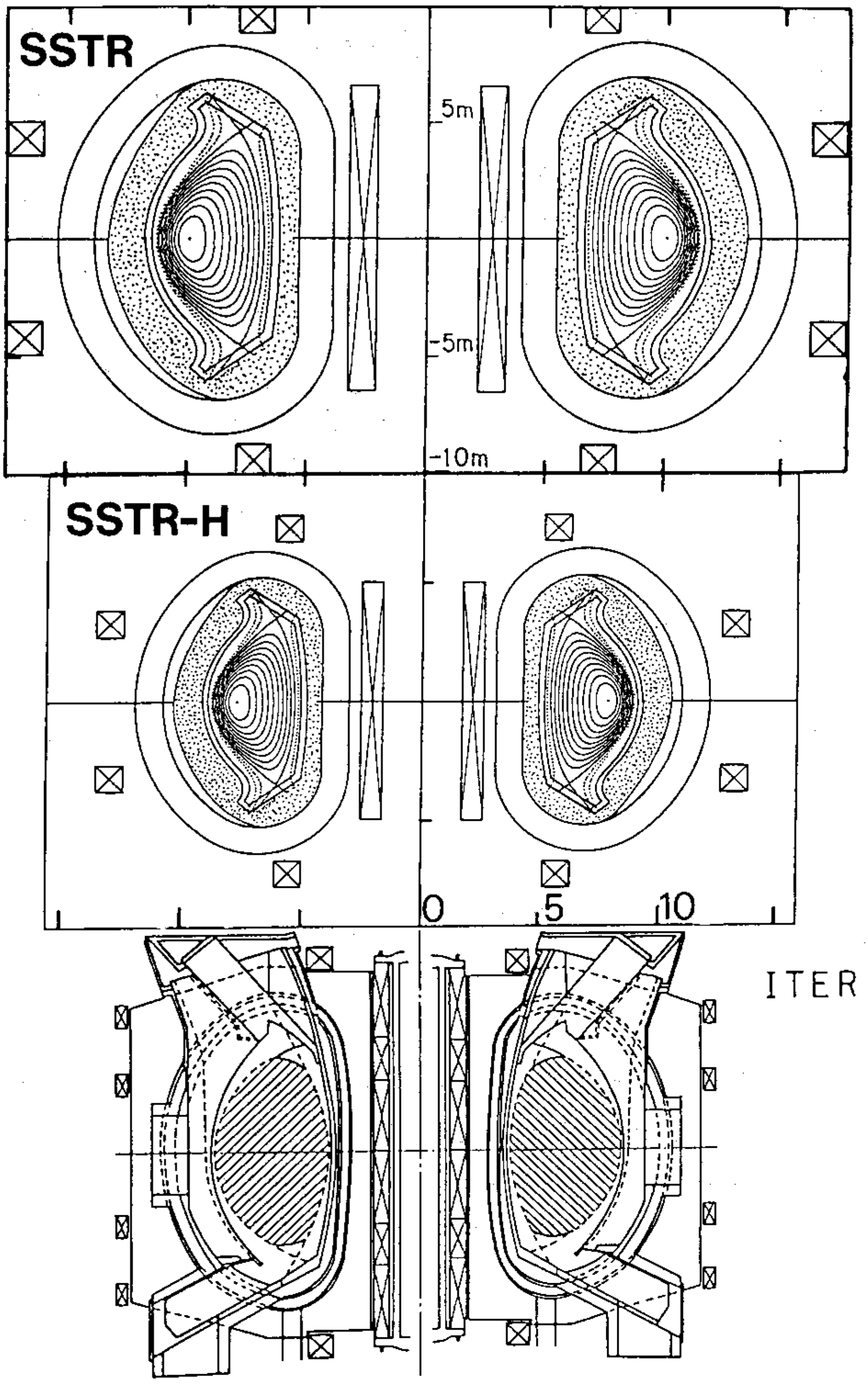

Fig. 8 Poloidal cross sections of the standard SSTR , compact SSTR and ITER. The toroidal field coil for the standard design is same as that of STARFIRE tokamak. The machine size is increased only in the major radius direction compared with the ITER device. The increase in the major radius strongly improves the plasma performance and reduce the required plasma current. The machne size can be reduced to 50% of that of the reference design if the maximum toroidal field is increased to 16T.

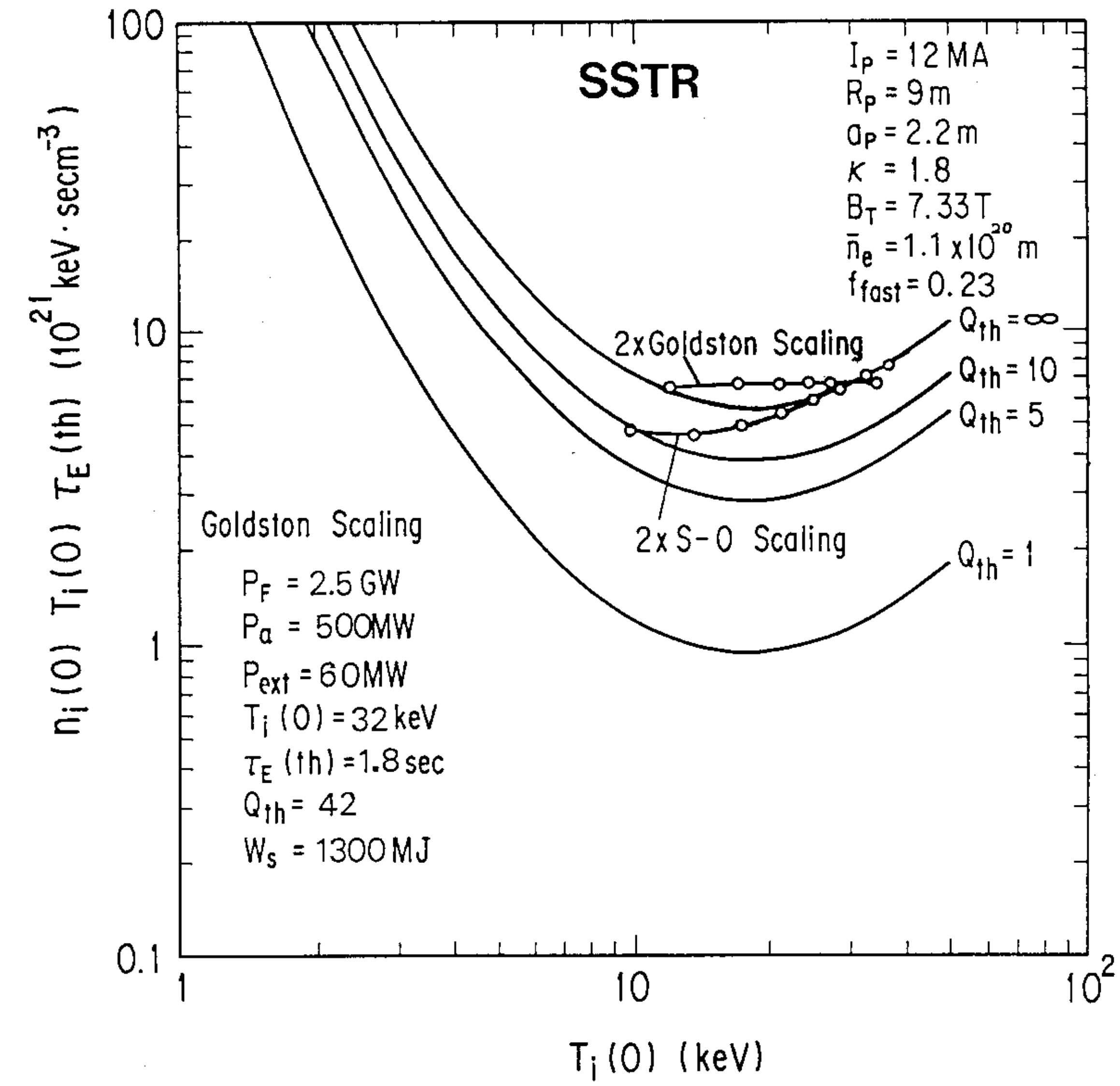

Fig.9 ($n_i(0)T_i(0)\tau_E$ (a), $T_i(0)$) diagram showing the confinement trace of the SSTR. Basic parameters are those given in Table 1. The confinement scalings of Goldston and Shimomura-Odajima with the confinement enhancement factor of 2.0 are used. The power requirement to the external heating system is consistent with that to the current driver.

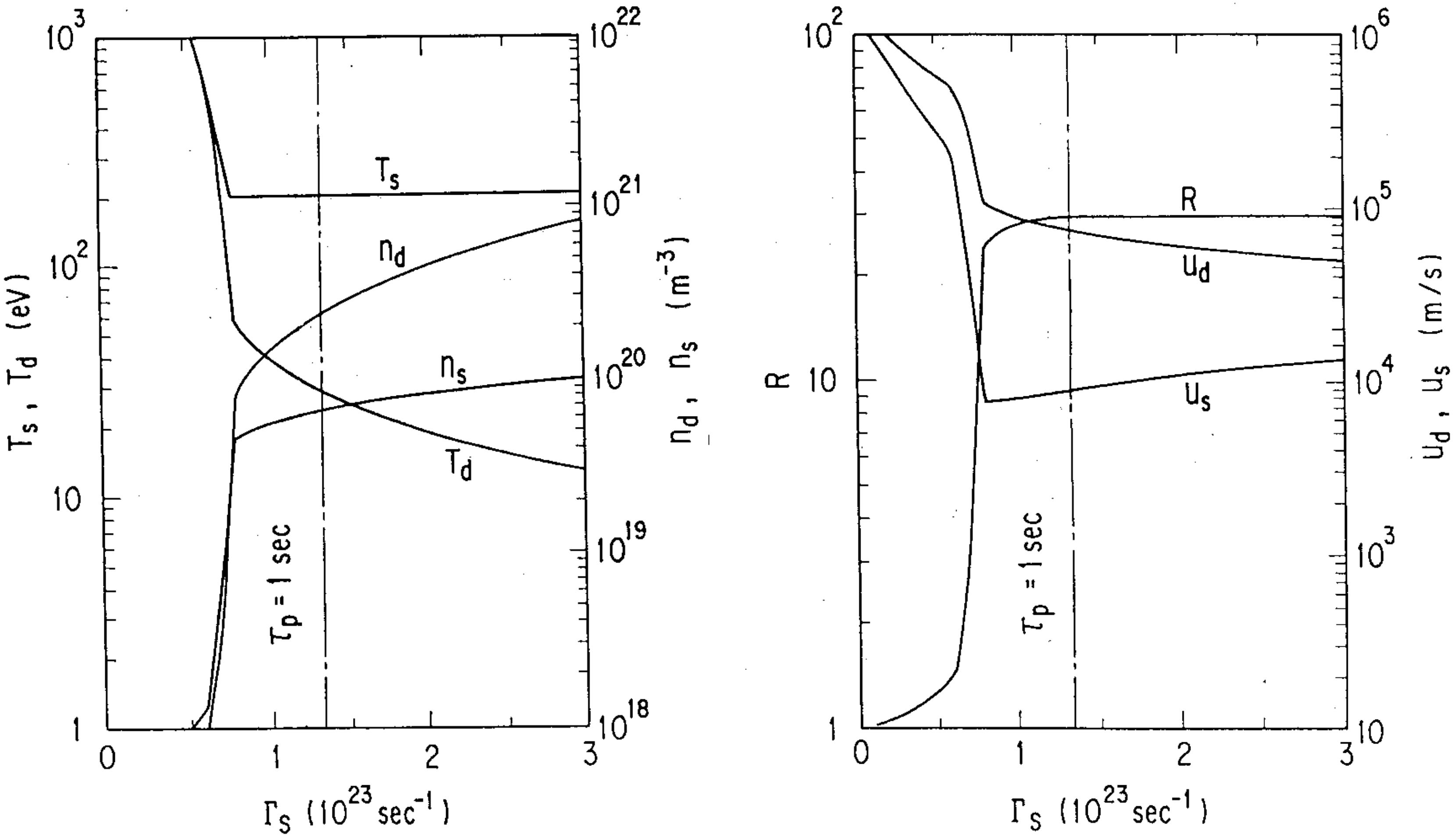

Fig. 10 The diverter and the scrape off parameters calculated with the two point diverter model as a function of the particle flux to the diverter for the reference SSTR given in Table 1. Detailed design of the diverter room must be made to assess the cold and dense diverter plasma condition.

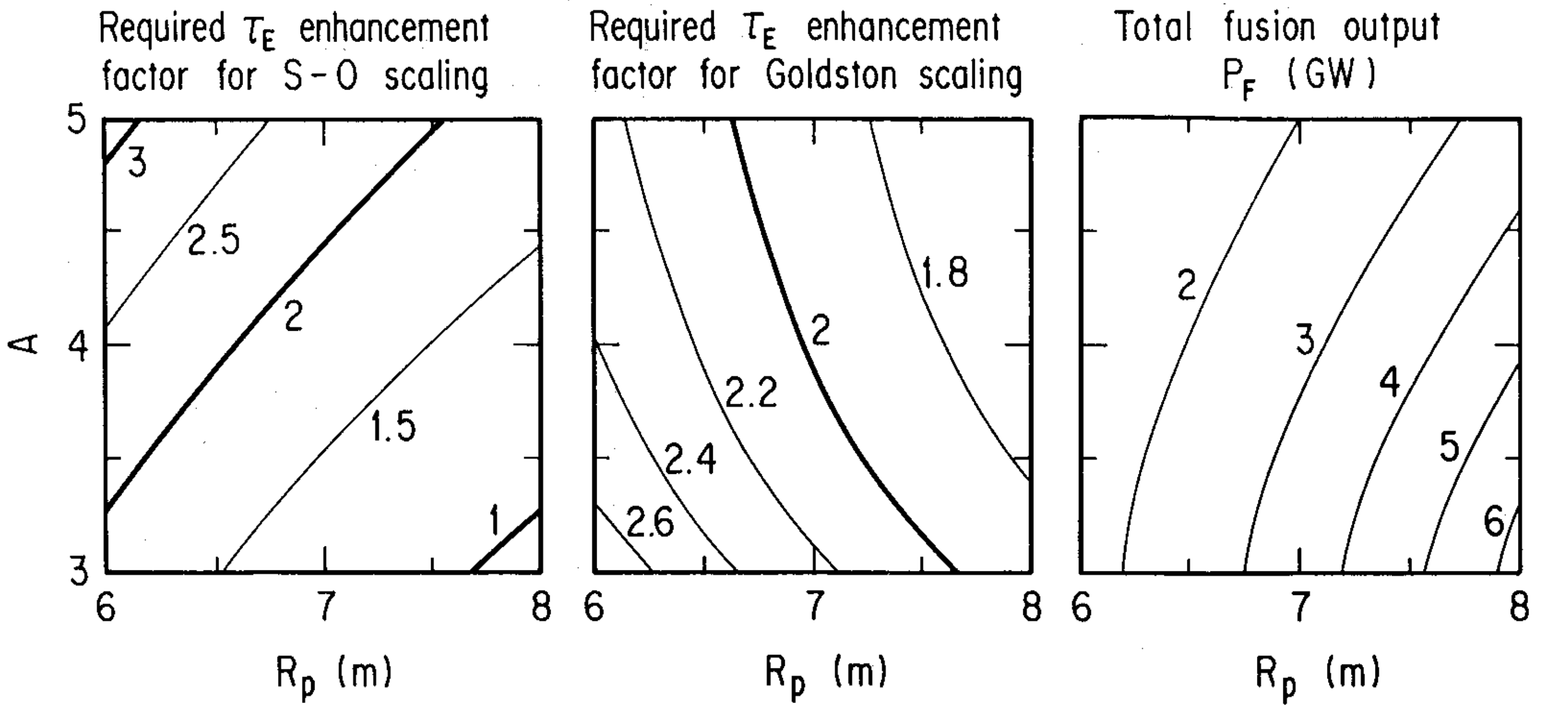

Fig. 11 Equi-contour plots of the required confinement enhancement factor and the total fusion output power as a function of the major radius and the aspect ratio for enhanced operation. The enhancement factor of 2 can be allowable for the major radius of 7 m for both scalings. The total fusion power is also significantly increased.

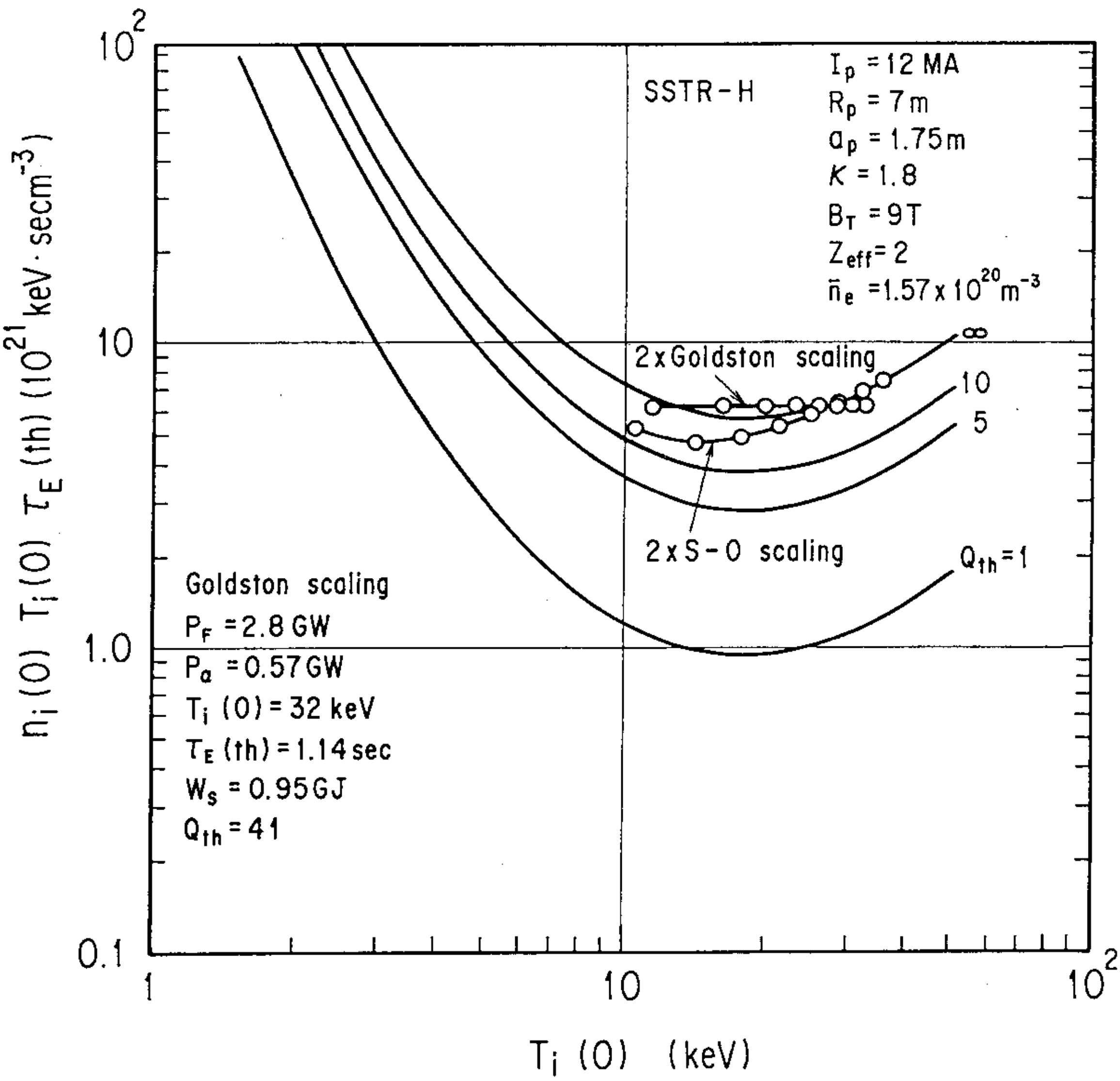

Fig. 12 (nτT,T) diagram showing the confinement predictions for Goldston and S-O scalings. The SSTR-H can reach high Q regime relavant for the steady state tokamak operation with relatively low plasma current with the confinement enhancement factor of 2.